doi:10.1093/brain/aww251 BRAIN 2016: 139; 3092–3108 | 3092

BRAIN
A JOURNAL OF NEUROLOGY

Prevention of vincristine-induced peripheral neuropathy by genetic deletion of SARM1 in mice

Stefanie Geisler,[1] Ryan A. Doan,[1] Amy Strickland,[2] Xin Huang,[2] Jeffrey Milbrandt[2,3] and Aaron DiAntonio[3,4]

Peripheral polyneuropathy is a common and dose-limiting side effect of many important chemotherapeutic agents. Most such neuropathies are characterized by early axonal degeneration, yet therapies that inhibit this axonal destruction process do not currently exist. Recently, we and others discovered that genetic deletion of SARM1 (sterile alpha and TIR motif containing protein 1) dramatically protects axons from degeneration after axotomy in mice. This finding fuels hope that inhibition of SARM1 or its downstream components can be used therapeutically in patients threatened by axonal loss. However, axon loss in most neuropathies, including chemotherapy-induced peripheral neuropathy, is the result of subacute/chronic processes that may be regulated differently than the acute, one time insult of axotomy. Here we evaluate if genetic deletion of SARM1 decreases axonal degeneration in a mouse model of neuropathy induced by the chemotherapeutic agent vincristine. In wild-type mice, 4 weeks of twice-weekly intraperitoneal injections of 1.5 mg/kg vincristine cause pronounced mechanical and heat hyperalgesia, a significant decrease in tail compound nerve action potential amplitude, loss of intraepidermal nerve fibres and significant degeneration of myelinated axons in both the distal sural nerve and nerves of the toe. Neither the proximal sural nerve nor the motor tibial nerve exhibit axon loss. These findings are consistent with the development of a distal, sensory predominant axonal polyneuropathy that mimics vincristine-induced peripheral polyneuropathy in humans. Using the same regimen of vincristine treatment in SARM1 knockout mice, the development of mechanical and heat hyperalgesia is blocked and the loss in tail compound nerve action potential amplitude is prevented. Moreover, SARM1 knockout mice do not lose unmyelinated fibres in the skin or myelinated axons in the sural nerve and toe after vincristine. Hence, genetic deletion of SARM1 blocks the development of vincristine-induced peripheral polyneuropathy in mice. Our results reveal that subacute/chronic axon loss induced by vincristine occurs via a SARM1 mediated axonal destruction pathway, and that blocking this pathway prevents the development of vincristine-induced peripheral polyneuropathy. These findings, in conjunction with previous studies with axotomy and traumatic brain injury, establish SARM1 as the central determinant of a fundamental axonal degeneration pathway that is activated by diverse insults. We suggest that targeting SARM1 or its downstream effectors may be a viable therapeutic option to prevent vincristine-induced peripheral polyneuropathy and possibly other peripheral polyneuropathies.

1 Department of Neurology, Washington University School of Medicine, Saint Louis, MO, USA
2 Department of Genetics, Washington University School of Medicine, Saint Louis, MO, USA
3 Hope Center for Neurological Diseases, Washington University School of Medicine, Saint Louis, MO, USA
4 Department of Developmental Biology, Washington University School of Medicine, Saint Louis, MO, USA

Correspondence to: Aaron DiAntonio,
Washington University School of Medicine, 4523 Clayton Ave. CB 8103
St. Louis, MO, 63110,
USA
E-mail: diantonio@wustl.edu

Received January 1, 2016. Revised July 27, 2016. Accepted August 16, 2016. Advance Access publication October 25, 2016

Correspondence may also be addressed to: Jeffrey Milbrandt, e-mail: jmilbrandt@wustl.edu

Keywords: SARM1; axonal degeneration; chemotherapy-induced peripheral neuropathy; vincristine; CIPN

Abbreviations: CNAP = compound nerve action potential; IENF = intraepidermal nerve fibre; VIPN = vincristine-induced peripheral neuropathy

Introduction

Peripheral neuropathies are the most common neurodegenerative diseases, affecting more than 20 million people in the USA alone and costing more than 12 billion US dollars annually. Although peripheral neuropathies can affect any peripheral nerve, they often start in the feet and hands and are characterized by dysaesthesias (such as burning and stabbing pain, feeling of 'pins and needles', and numbness), ataxia, distal weakness and autonomic symptoms, including constipation and orthostatic hypotension. Many neuropathies are caused by degeneration of long axons, yet the mechanisms that lead to this destruction remain poorly understood and no therapies exist that directly target axonal degeneration. Development of such therapies would have enormous societal impact and benefit many patients.

A common cause of peripheral neuropathy is treatment with chemotherapeutic drugs. Chemotherapy-induced peripheral neuropathies (CIPN) are often sensory predominant, but may also lead to weakness, necessitating 'chemoholidays' or switching of the chemotherapeutic regimen (Argyriou *et al.*, 2014; Ezendam *et al.*, 2014; Carozzi *et al.*, 2015; Costa *et al.*, 2015; Jongen *et al.*, 2015). Unlike most other side-effects of chemotherapeutic agents, CIPN may last long after the cancer treatment has ended and cause permanent disability. Therefore, treatments that prevent CIPN would improve (i) cancer treatment by allowing more aggressive drug dosing; and (ii) the quality of life of cancer survivors both during and after treatment. CIPN is an especially attractive target for the development of neuroprotective therapies because the timing of the toxic insult is known, permitting candidate drugs to be co- or pre-administered before nerve injury.

Tremendous progress has been made in recent years unravelling mechanisms of acute axonal degeneration after nerve cut or crush. Studies of Wallerian degeneration, as this form of axonal degeneration after traumatic insult is known, revealed that axons do not die passively due to lack of cell-body derived nutrients, but activate a genetically encoded axonal self-destruction program that leads to rapid axonal fragmentation after a long period of relative latency (Wang *et al.*, 2012; Gerdts *et al.*, 2016). The discovery of Wallerian degeneration slow (*Wlds*) mutant mice, in which axonal degeneration is greatly delayed after traumatic injury, revealed that axonal degeneration indeed can be blocked (Lunn *et al.*, 1989). However, *Wlds* mice harbour a spontaneous mutation that results in the expression of a gain-of-function fusion protein that does not normally exist (Coleman *et al.*, 1998; Mack *et al.*, 2001; Araki *et al.*, 2004), limiting the therapeutic utility of this discovery. Until recently, no loss-of-function mutants were identified that had similar axon protective properties. We and others recently discovered sterile alpha and TIR motif-containing protein 1 (SARM1) as an essential component of this endogenous axonal self-destruction pathway (Osterloh *et al.*, 2012; Gerdts *et al.*, 2013, 2015). Whereas axons of wild-type mice degenerate within 3 days after sciatic nerve cut, severed axons of SARM1 knockout mice remain intact for >2 weeks. Conversely, activation of SARM1 is sufficient to induce axonal degeneration in healthy axons (Gerdts *et al.*, 2013, 2015). This identifies SARM1 as the central executioner of acute axonal destruction and fuels hope that targeting SARM1 or its downstream effectors can be used therapeutically.

Recent studies are identifying the molecular mechanisms by which SARM1 triggers axon degeneration (Gerdts *et al.*, 2013; Yang *et al.*, 2015). At rest SARM1 is held in an inactive state, and on axon injury, this autoinhibition is relieved thereby triggering SARM1 activity (Gerdts *et al.*, 2013). Activated SARM1 induces the rapid destruction of the essential metabolic co-factor nicotinamide adenine dinucleotide (NAD^+), inducing metabolic collapse and axon death (Gerdts *et al.*, 2015). Importantly, SARM1 is predominantly expressed in the central and peripheral nervous system of mammals (Kim *et al.*, 2007; Chen *et al.*, 2011), and SARM1 knockout mice are viable, fertile and grossly normal (Lin and Hsueh, 2014). Hence, SARM1 or its downstream effectors may be excellent targets for the development of axoprotective therapies.

SARM1 is required for acute axonal degeneration after nerve cut, but axon loss in most neuropathies, including chemotherapy-induced neuropathy, is the result of subacute/chronic processes that may engage different injury responses than axotomy. After nerve transection, there is a long latent period after which all axons distal to the cut degenerate nearly simultaneously (Beirowski *et al.*, 2005). In contrast, only a few axons degenerate at any given time in most neuropathies, with degeneration of short axonal segments that proceeds slowly from distal to proximal. It is not known whether SARM1 promotes axonal degeneration in these more chronic conditions; however, studies of *Wlds* mice suggest that this may be the case. *Wlds* mice not only show greatly delayed axonal degeneration after traumatic injury, but also exhibit reduced axon loss after acute treatment with the chemotherapeutic agent Taxol

(Wang *et al.*, 2002). Moreover, neurites from *Wlds* mice transiently exposed to the chemotherapeutic drug vincristine resist axonal degeneration in dorsal root ganglia cultures (Wang *et al.*, 2001). Excitingly, we and others recently revealed that vincristine-induced neurite degeneration is also significantly delayed in dorsal root ganglion cultures obtained from SARM1 knockout mice (Gerdts *et al.*, 2013; Yang *et al.*, 2015). These findings motivated us to assess whether genetic deletion of SARM1 decreases axonal degeneration in a mouse model of vincristine-induced neuropathy.

Vincristine is widely used to treat haematological cancers, such as leukaemias and lymphomas, and solid tumours, including brain tumours, neuroblastoma, Wilms tumour, rhabdomysarcoma, Ewing sarcoma and retinoblastoma (Diouf *et al.*, 2015). Vincristine is an effective chemotherapeutic because it inhibits tubulin polymerization (Himes *et al.*, 1976; Owellen *et al.*, 1976), thereby blocking mitotic spindle formation and preventing cell division. However, disrupting tubulin polymerization also interferes with anterograde and retrograde axonal transport (LaPointe *et al.*, 2013), which likely triggers neuropathy. Neuropathy may affect up to 80% of patients treated with vincristine and is the main dose-limiting side effect (DeAngelis *et al.*, 1991; Haim *et al.*, 1994; Reinders-Messelink *et al.*, 2000; Lavoie Smith *et al.*, 2015). In adult patients, vincristine-induced neuropathy is a sensory predominant distal axonopathy (Casey *et al.*, 1973; Verstappen *et al.*, 2005). Here, we generated a model of a distal sensory neuropathy using female and male mice. We show that SARM1 knockout prevents the degeneration of intraepidermal nerve fibres as well as myelinated axons in the toe and distal sural nerve and improves functional outcomes, preserving normal nerve conduction and blocking the development of mechanical and heat hyperalgesia. Thus, SARM1 is required for the development of vincristine-induced peripheral neuropathy (VIPN) in the mouse. The demonstration that the endogenous SARM1 axonal degeneration pathway mediates axon loss in distal axonopathies suggests that the SARM1 pathway may have a broader role in neurodegenerative diseases characterized by subacute axon loss. We propose that targeting the SARM1 pathway may be a viable therapeutic option to prevent the development of chemotherapy-induced neuropathies such as VIPN and should be investigated as a candidate treatment for neurodegenerative diseases involving chronic axon loss.

Materials and methods

Animals and vincristine injections

All procedures were approved by the Washington University of Saint Louis Medical School Institutional Animal Care and Use Committee (Protocol #20150043). This manuscript was prepared in adherence to the ARRIVE guidelines.

Several treatment protocols to induce VIPN in mice have been described, but the results are conflicting. Therefore, in pilot experiments, we used wild-type mice (C57Bl/6 mice own colony) to systematically test different treatment regimens. Vehicle [sterile phosphate-buffered saline (PBS)] or vincristine (Sigma) dissolved in sterile PBS (0.5 mg/ml) was administered intraperitoneally at a dose of 1 mg/kg, 2 mg/kg and 3 mg/kg weekly as well as 1.5 mg/kg and 1.7 mg/kg twice weekly. In addition, we evaluated SARM1 knockout mice on the C57Bl6/J background that received vincristine injections at 1 mg/kg and 3 mg/kg weekly as well as 1.5 mg/kg and 1.7 mg/kg twice weekly. There was not a linear response to the cumulative dose, but the effects of vincristine depended on the size of individual doses and frequency of administration. At all dosages tested, we observed a similar weight loss and mortality between wild-type and SARM1 knockout mice (Supplementary Fig. 1). Weekly vincristine injections of 1 mg/kg were well tolerated, but did not cause axon loss in wild-type mice that was reliably reproduced. Mice receiving intraperitoneal injections of 1.7 mg/kg twice weekly as well as 2 mg/kg or 3 mg/kg weekly, had a high mortality. Although 1.5 mg/kg twice weekly has the same cumulative dose as 3 mg/kg weekly, it was better tolerated and induced neuropathy in wild-type mice that was reliably reproduced between cohorts.

We therefore chose a vincristine dose of 1.5 mg/kg twice weekly, and treated mice as follows: $Sarm1^{+/-}$ males and females on the C57Bl6/J background (Jackson laboratories) were bred to obtain age matched male and female $Sarm1^{-/-}$ ($n = 40$; 14 male, 26 female) and $Sarm1^{+/+}$ ($n = 26$; nine males, 17 females) littermate mice. In addition, 14 age and gender (nine males, five females) matched C57Bl6/J mice were used as wild-type controls. There was no difference between $Sarm1^{+/+}$ littermate and age and gender-matched C57Bl6/J controls. All animals were socially housed on a 12 h light dark cycle with water and food *ad libitum*. Behavioural tests and nerve conduction studies were performed 1 week before the first vincristine injection and 1 week after the last. Weight was measured daily. If a mouse lost more than 0.5 g weight from the day before, it received sterile 0.9% saline intraperitoneally.

Approximately 20-week-old wild-type (19.3 ± 0.6 weeks, range 12–31 weeks) and SARM1 knockout mice (20.7 ± 0.6 weeks, range 12–31 weeks) were injected intraperitoneally with 1.5 mg/kg vincristine dissolved in 0.5 mg/ml sterile PBS (wild-type $n = 29$; SARM1 knockout $n = 30$) or vehicle (sterile PBS; wild-type $n = 11$, SARM1 knockout $n = 10$) at the same volume twice weekly. Of 29 wild-type and 30 SARM1 knockout mice injected with 1.5 mg/kg vincristine twice weekly, five wild-type and six SARM1 knockout mice died before the end of the experiment and were excluded from analysis. No vehicle-treated mouse died during the experiment. There was no significant difference in the average weight between treatment groups at baseline [vehicle-treated wild-type 24.8 ± 0.9 g, $n = 11$; vincristine-treated wild-type 24.5 ± 0.8 g, $n = 23$; vehicle-treated SARM1 knockout 23.4 ± 0.8 g, $n = 10$; vincristine-treated SARM1 knockout 23.2 ± 0.5 g, $n = 24$; one-way ANOVA $F(3,64)$ $P = 0.41$]. After the first injection, both vincristine and vehicle-treated wild-type and SARM1 knockout mice lost weight (Supplementary Fig. 2), possibly due to stress associated with the injection. All groups recovered weight before the second injection. At the end of the

experiment both vincristine-treated wild-type and SARM1 knockout mice showed a similar modest weight loss of 6% ± 2% and 7% ± 1%, respectively ($P < 0.01$ for wild-type and $P < 0.001$ for SARM1 knockout). Despite the weight loss, both wild-type and SARM1 knockout mice continued to be active and showed normal grooming behaviour. In addition to weight loss, two wild-type and one SARM1 knockout mouse developed mild hair loss.

Nerve conduction studies

Two days before the first injection and 7 days after the last vehicle or vincristine injection, mice were anaesthetized using a mixture of 4% isoflurane and 2.5 l oxygen for induction of anaesthesia and 2% isoflurane with 2.5 l oxygen for maintenance. Recording electrodes (platinum subdermal EEG electrodes, 0.4 mm diameter, 12 mm length; Viasys) were placed subcutaneously at the base of the tail and stimulating electrodes were inserted 30 mm distal from the negative recording electrode. The ground electrode was placed between stimulating and recording electrodes. Evoked compound nerve action potentials (CNAPs) were obtained using a Viking Quest electromyography machine (Nicolet). Square wave pulses of 0.1 ms duration were applied and intensity was increased until a maximal response was achieved. The intensity was increased 20% further to obtain supramaximal stimulation and responses to 20 stimuli were averaged. Amplitude was measured from baseline to first peak and conduction velocity calculated as a function of distal latency and distance between stimulating and recording electrode (30 mm). The experimenter was blind to treatment and genotype.

Behavioural studies

For behavioural studies, all mice (wild-type $n = 12$, all littermate controls; SARM1 knockout $n = 16$) received vincristine and were tested 1 week before and 1 week after the last vincristine injection. The order in which the experiments were performed was identical before and after vincristine treatment. The experimenters were blind to the genotype.

Von Frey

Mice were habituated individually in 10 × 10 × 15 cm open Plexiglass boxes with perforated lids on wire mesh for 4 h. After mice stopped exploring and were resting, von Frey testing was performed according to the up-down method (Chaplan *et al.*, 1994). Briefly, the middle of the plantar surface of the hind paw between the footpads was stimulated for 2 s with a filament (Semmes-Weinstein monofilaments, Stoelting), starting with a bending force of 0.32 g. If the mouse withdrew the foot, the next lower filament was taken. If the mice did not withdraw the hindpaw, it was stimulated with the next higher filament. This was repeated four more times after the first change in response. Right and left hind paws were tested separately. The withdrawal threshold was calculated according to Dixon (1980) and the withdrawal between right and left foot for each mouse averaged. Von Frey experiments in the beginning and at the end of the experiment were done at the same time of the day.

Analgesia meter

After acclimating in the test room, mice were placed individually on the hotplate analgesia meter (Columbus instruments), which was surrounded by a Plexiglass frame. After 10 min, the temperature was gradually increased at a constant rate from 31°C to 51°C. Once the mouse elevated and licked the hindpaw, the recording was stopped via a foot switch and the temperature recorded. The highest temperature at which a mouse licked a paw was 42.9°C.

Rotarod

After acclimating in the test room, mice were placed on the rotarod (Columbia Instruments Rotamex 5) at constant speed (one rotation per minute; rpm) for 5 min. This was followed by an acceleration of 3 rpm every 10 s. Subsequently mice were tested at a constant speed of 2 rpm. The experiment was stopped after 60 s for constant speed and 360 s for accelerating rotarod or when the mouse fell down, whichever came first. Every mouse was tested five times on both the accelerating and constant speed rotarod, with at least 10 min of rest time between. Results of the five tests were averaged.

Inverted screen

Mice were placed on a vertical wire mesh screen, which was then inverted so that the mice hang upside down. The test was ended after 180 s or when the mouse fell off the screen, whichever came first. Each mouse was tested three times, resting at least 30 min between each trial, and the times of the three trials were averaged.

Tissue preparation

Twelve days after the last vincristine or vehicle injection, mice were deeply anaesthetized by isoflurane inhalation and euthanized by cervical dislocation. The third right toe was obtained and the right sciatic, sural and tibial nerves were immediately dissected out, and fixed by immersion in freshly prepared 3% glutaraldehyde in 0.1 M PBS over night at 4°C. The plantar surface of the right foot was removed and fixed in freshly prepared Zamboni's fixative (0.12% picric acid, 2% paraformaldehyde in 0.1 M PBS, pH 7.4) over night at 4°C.

Toluidine blue staining and axon quantification

Nerves were rinsed in 0.1 M Sorensen's phosphate buffer (SPB), incubated in 1% osmium tetroxide (Sigma) in 0.1 M phosphate buffer over night at 4°C, washed in 0.1 M SPB and dehydrated through a graded series of ethanol followed by a 50%/50% ethanol/propylene oxide solution, and 100% propylene oxide. Nerves were then placed into ascending mixtures of araldite/propylene oxide solutions (50:50, 70:30, 90:10), and embedded in 100% araldite at a ratio of 12:9:1 (araldite:DDSA:DMP30; Electron Microscopy Sciences) and polymerized overnight at 60°C. Nerve cross-sections (400 nm thick) were cut using a Leica EM UC6 or UC7 ultramicrotome, and stained with 1% toluidine blue (Fisher Scientific). Sections were imaged using a 100× oil immersion objective on a Leica DMI 4000B microscope. To analyse axon number and axon density of the distal sural, proximal sural and tibial nerves, photographs were stitched in Adobe Illustrator so that the entire cross-section of the nerve was included. All axons per cross-section were counted in ImageJ. The area

of individual axons of the distal sural nerve was measured using Leica's Application Suite X. To analyse numbers of degenerating axons in the toes, axons with disrupted myelin or myelin clumps and dark or pale homogeneous axoplasm without discernible mitochondria as well as large axons with dark cytoplasm and no discernible myelin sheath were counted as degenerating axons. All analysis was done with the samples blinded to the observer.

Electron microscopy

Selected blocks of nerves used to cut 400-nm thick semithin sections were used to cut 60-nm thick ultrathin sections using a Leica EM UC6 and stained with uranyl acetate and lead citrate. Electron microscopy images were obtained with a JEOL JEM 1400 TEM.

Immunohistochemistry and determination of intraepidermal nerve fibre density

Footpads were thoroughly rinsed in PBS and immersed in 30% sucrose overnight at 4°C. They were then frozen in O.C.T. (Tissue Tec) in liquid 2-methylbutane cooled by dry ice. Four adjacent series of 50-µm thick cross-sections were cut at the cryostat (Leica CM1860) and collected such that the entire plantar surface was sampled at 200 µm intervals. Series of sections were stored prior to processing at −20°C in a cryoprotectant comprising 30% sucrose and 33% ethylene glycol in SPB.

A series of sections was thoroughly rinsed in 0.1 M SPB, immersed in 10% normal goat serum (NGS) and 0.1% Triton™ X-100 in PBS (PBS-T) for 1 h, and transferred into rabbit anti-Protein Gene Product 9.5 (1:1000, EMD Millipore) overnight at 4°C. The next day, sections were thoroughly rinsed in PBS-T and placed in Cy3-conjugated goat anti-rabbit secondary antibody (Invitrogen) at a dilution of 1:500. After further rinsing, sections were mounted on gelled slides and coverslipped using Vectashield with DAPI (Vector Laboratories) to allow visualization of nuclei.

The part of the plantar surface containing the footpad was identified and imaged on a Leica DMI 4000B confocal microscope using a 20× oil objective and a Leica DFC 7000-T camera. Intraepidermal nerve fibres (IENFs) crossing into the epidermis over the entire medial lateral extension of the footpad were determined by examining the entirety of the 50 µm stack using Leica Application Suite X. Axons that crossed the basement membrane were counted, whereas secondary branching and epidermal nerve fragments that do not cross the basement were not (Ebenezer *et al.*, 2007). The length of epidermis was measured at the level of the basement membrane and the density of IENFs (IENFs/mm) was obtained. IENF densities were averaged in three separate sections for each animal. Imaging and analysis was done with the samples blinded to the observer.

Photomicrographs

Brightfield images were obtained with a Leica DMI 4000B using a 100× oil objective and Leica DFC 7000-T Camera. Minor adjustments of brightness and contrast of the entire photomicrographs were made in Photoshop. *Z*-stack images of IENF fibres were obtained in the confocal mode of the Leica DMI 4000B using a 40× oil objective. No post-processing was performed on the confocal images.

Statistical analysis

Unless otherwise stated, data are reported as means ± standard error of the mean (SEM). Between group comparisons were made with one way and two-way ANOVA or unpaired *t*-test as appropriate. Two-sided significance tests were used throughout and $P < 0.05$ was considered statistically significant. All statistics were calculated with the aid of Prism software.

Results

Genetic deletion of SARM1 robustly protects axons from degeneration after acute injuries (Osterloh *et al.*, 2012; Gerdts *et al.*, 2013; Massoll *et al.*, 2013; Henninger *et al.*, 2016). However, axon loss in many neurodegenerative diseases, including most neuropathies, is protracted and it is unknown whether SARM1 mediates axonal degeneration in these conditions. To determine if SARM1 knockout also protects from gradual axonal degeneration we generated a mouse model of vincristine induced neuropathy and assayed for numbers of intraepidermal nerve fibres of the footpad and of myelinated axons in sensory and motor peripheral nerves at different distal-proximal levels in wild-type and SARM1 knockout mice. We further assessed functional outcomes via nerve conduction studies and sensory-motor assays, including von Frey, analgesia meter, rotarod and inverted screen.

A mouse model of vincristine-induced peripheral neuropathy

The severity of VIPN in patients depends on dose intensity and total cumulative dose whereby higher individual and cumulative doses are associated with more severe neuropathy (Sandler *et al.*, 1969; Casey *et al.*, 1973; Verstappen *et al.*, 2005). Of several published treatment regimens to induce VIPN in mouse, few were evaluated for axonal degeneration and results between studies are conflicting (Tanner *et al.*, 1998*a*; Topp *et al.*, 2000; Bruna *et al.*, 2011; Boehmerle *et al.*, 2014). Therefore, in pilot experiments, we systematically evaluated different treatment regimens (described in detail in the 'Materials and methods' section; Supplementary Fig. 1 and 2). We chose a vincristine dose of 1.5 mg/kg twice weekly as it was moderately well tolerated (Supplementary Fig. 2) and caused axon loss in wild-type animals that was reliably reproduced among cohorts.

SARM1 knockout protects from loss of intraepidermal nerve fibres after vincristine

Many neuropathies are characterized by degeneration of small IENFs. IENFs consist predominantly of unmyelinated C-fibres and to a lesser extent of thinly myelinated A delta fibres both of which convey pain and temperature information. Pain and changes in temperature perception occur commonly in VIPN and can persist long after cessation of treatment (Boyette-Davis *et al.*, 2013). Hence, changes in IENFs likely occur in human VIPN. Therefore, to evaluate whether SARM1 knockout prevents axon loss in murine VIPN we analysed the IENF densities of the footpad. Sections were stained with the pan-axonal marker protein gene product 9.5 (PGP9.5; Fig. 1), and IENF were counted as they crossed into the counterstained epidermis (Fig. 1A) using established counting rules (Ebenezer *et al.*, 2007). In wild-type and SARM1 knockout vehicle-treated mice, IENFs were morphologically similar and ascended as straight fibres within the epidermis to superficial layers of the stratum spinosum (Fig. 1B and E). Vehicle-treated SARM1 knockout mice had a slightly higher IENF density than wild-type mice (59 mm ± 3 SARM1 knockout versus 55 ± 3 mm wild-type; Fig. 1D), but this difference was not statistically significant ($P = 0.37$, unpaired *t*-test, $n = 8$–9). In vincristine-treated wild-type mice, we observed a significant decrease of IENF density (Fig. 1C and D; $P < 0.05$). In addition, many intraepidermal axons were shorter in vincristine than in vehicle-treated mice and did not extend to the superficial layers of the stratum spinosum (Fig. 1C) consistent with a 'dying back' axonal degeneration in wild-type mice. In contrast, there was no difference in the IENF density between vehicle and vincristine-treated SARM1 knockout mice (Fig. 1D–F). Strikingly, despite vincristine treatment, IENFs in SARM1 knockout extended into the superficial layers of the stratum spinosum (Fig. 1F), indicating remarkable fibre preservation in SARM1 knockout mice. These results demonstrate that loss of SARM1 prevents degeneration of IENF in vincristine-induced neuropathy.

SARM1 knockout prevents vincristine-induced loss of myelinated axons in distal sensory nerves

We next assessed whether SARM1 knockout prevents loss of myelinated axons. Because vincristine induced neuropathy in patients is sensory predominant and symptoms start distally in the hands and feet, we analysed semithin sections of distal sensory nerves, i.e. the sural nerve and nerves of the toe.

The sural nerve was chosen for analysis because it is commonly used in human diagnostic biopsies and descriptions of human pathology in VIPN have been published (Gottschalk *et al.*, 1968; Bradley *et al.*, 1970). We first assessed whether there are differences between vehicle-treated SARM1 knockout and wild-type sural nerves. The branching pattern of the distal sural nerve is variable and therefore the nerve can be comprised of one to four fascicles, but usually consists of either one large fascicle or two small ones. The fascicle sizes were the same between SARM1 knockout and wild-type mice (Supplementary Fig. 3A). Cross-sections of the distal sural nerve did not appear appreciably different. Large and small myelinated axons were of similar shape, size, and had a similar distribution within the nerves in wild-type and SARM1 knockout mice (Fig. 2A and D). There was no difference in axon density, axon size distribution and G-ratio between wild-type and SARM1 knockout mice (Supplementary Fig. 3B–D).

In vincristine-treated wild-type mice, some myelinated axons exhibited morphological signs of axonal degeneration (Fig. 2B and C) and myelinated axons appeared less densely packed (Fig. 2B). In contrast, vincristine-treated SARM1 knockout sural nerves looked similar to vehicle-treated SARM1 knockout nerves (Fig. 2D–F). To assess for axon loss, we stitched light microscopic images taken at 100× magnification and counted all myelinated axons in the entire cross-section of the sural nerve, thereby avoiding potential selection bias. The mean axon density in vincristine-treated wild-type mice was significantly lower than in vehicle-treated wild-type mice and vincristine-treated SARM1 knockout mice (Fig. 2H, $P < 0.05$). There was no difference in axon density between vehicle-treated and vincristine-treated SARM1 knockout mice (Fig. 2H). To evaluate whether vincristine causes a preferential loss of certain fibre types we used Leica Application Suite-X software-based thresholding and automated axon area measurements to assess the number of axons of different diameters. We observed significantly fewer small myelinated axons in the sural nerves of vincristine as compared to vehicle-treated wild-type mice (Fig. 2I; $P < 0.05$). This finding may be due to loss of the small myelinated axons or swelling of all axons causing a right-shift of the histogram as reported in another animal model of VIPN (Tanner *et al.*, 1998*a*; Topp *et al.*, 2000). However, we did not detect a right shift of axon diameters (Fig. 2I), suggesting that the significantly lower number of small myelinated axons in vincristine-treated wild-type mice is due to axon loss. In contrast, there was no difference in axon size distribution between vehicle and vincristine-treated SARM1 knockout mice (Fig. 2J), further supporting the finding that SARM1 knockout mice are protected from axon loss.

In the later stages of Wallerian degeneration, macrophage infiltration may be observed. To evaluate if macrophage infiltration occurs in our model, we analysed cross-sections of frozen distal sural nerves immunostained with the macrophage marker anti-CD68 (Supplementary Fig. 4A). There was no significant difference in the numbers of macrophages between wild-type and SARM1 knockout mice at baseline or between vehicle and vincristine-treated wild-type or SARM1 knockout mice (Supplementary Fig. 4B) indicating that macrophage infiltration does not play

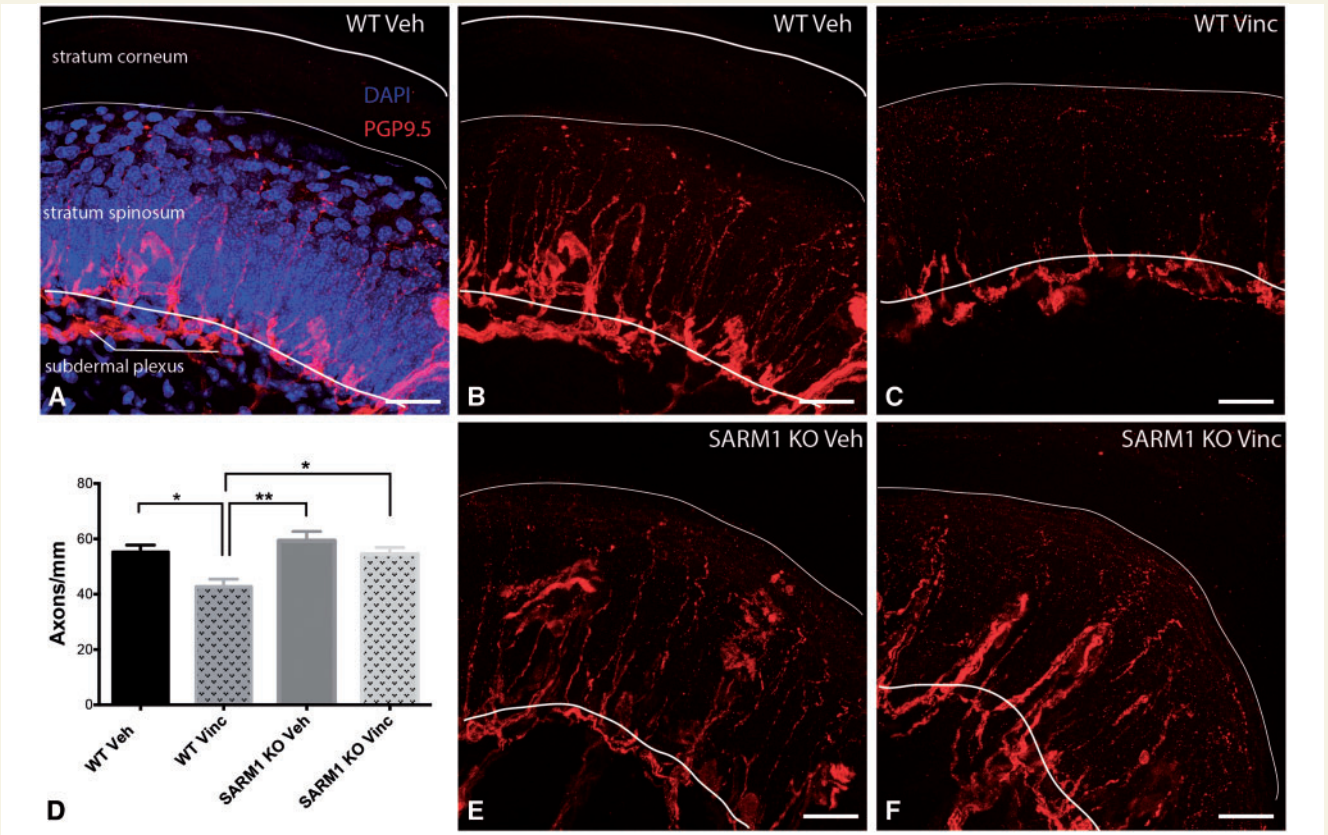

Figure 1 SARM1 knockout blocks vincristine-induced degeneration of IENF. (**A**) IENFs stained with the pan-axonal marker PGP 9.5 (red) extend at a ~90° angle from the subdermal plexus into the stratum spinosum of the epidermis (nuclei stained with DAPI in blue). (**B**) Same image as **A**, without overlay of the epidermis. Note that IENF extend into superficial layers of the stratum spinosum. (**C**) In vincristine-treated wild-type mice fewer fibres cross into the epidermis and many IENFs appear short. (**D**) Quantification of IENF density. There are significantly fewer IENFs in vincristine-treated wild-type mice as compared to vehicle-treated wild-type and SARM1 knockout mice as well as SARM1 knockout treated vincristine mice. Data are presented as mean ± SEM [one-way ANOVA, $F(3,41) = 6.870$; $P = 0.0007$; *post hoc* Tukey's; $^{*}P < 0.05$; $^{**}P < 0.01$; $n = 8$–9 for vehicle-treated wild-type (WT Veh) and SARM1 knockout (SARM1 KO Veh) mice and $n = 14$ for vincristine-treated wild-type (WT Vinc) and SARM1 knockout mice (SARM1 KO Vinc)]. For clarity in the figure, only significant results are indicated. (**E**) IENFs in vehicle-treated SARM1 knockout mice look similar to IENFs in vehicle-treated wild-type mice (**B**). (**F**) Representative image of IENFs in vincristine-treated SARM1 knockout mice. Note that many fibres cross into the epidermis and extend to the superficial layers of the stratum spinosum. Scale bar = 25 μm.

a prominent role in our model of vincristine-induced neuropathy. This is in accord with published findings in human studies of VIPN (Gottschalk *et al.*, 1968) and other distal symmetric non-vasculitic peripheral polyneuropathies (Uceyler *et al.*, 2016).

VIPN has been postulated to be a dying back neuropathy based on results of nerve conduction studies showing decreased nerve amplitudes distally but not proximally (Guiheneuc *et al.*, 1980). However, a study evaluating rat saphenous nerves found no differences in nerve pathology between distal and proximal parts of the nerve (Gottschalk *et al.*, 1968). To evaluate whether axon loss is uniform or distally predominant in our model, we analysed the sural nerve at the level of the knee. In the proximal sural nerve, we did not observe significant differences in axon numbers between vincristine and vehicle-treated wild-type and SARM1 knockout mice (Fig. 2G). There was a trend towards slightly fewer axons in the vehicle-treated SARM1 knockout mice than in vehicle-treated wild-type mice, but this difference was not statistically significant (Fig. 2G; SARM1 knockout 334.7 ± 44, $n = 7$; wild-type 411.1 ± 45.3, $n = 8$; $P = 0.26$, unpaired *t*-test). When we compared the number of axons from the same sural nerve at proximal and distal sural locations, we observed significantly fewer axons distally in wild-type vincristine-treated mice (Fig. 2G, $P < 0.001$). Thus, the axon loss in the VIPN model is distal predominant, which fits well with the distal predominant symptoms in human VIPN. In contrast, axon numbers were not significantly different between proximal and distal sural nerves in vehicle-treated wild-type mice and vehicle and vincristine-treated SARM1 knockout mice. Hence, genetic deletion of SARM1 prevents distal degeneration of myelinated axons of the sural nerve.

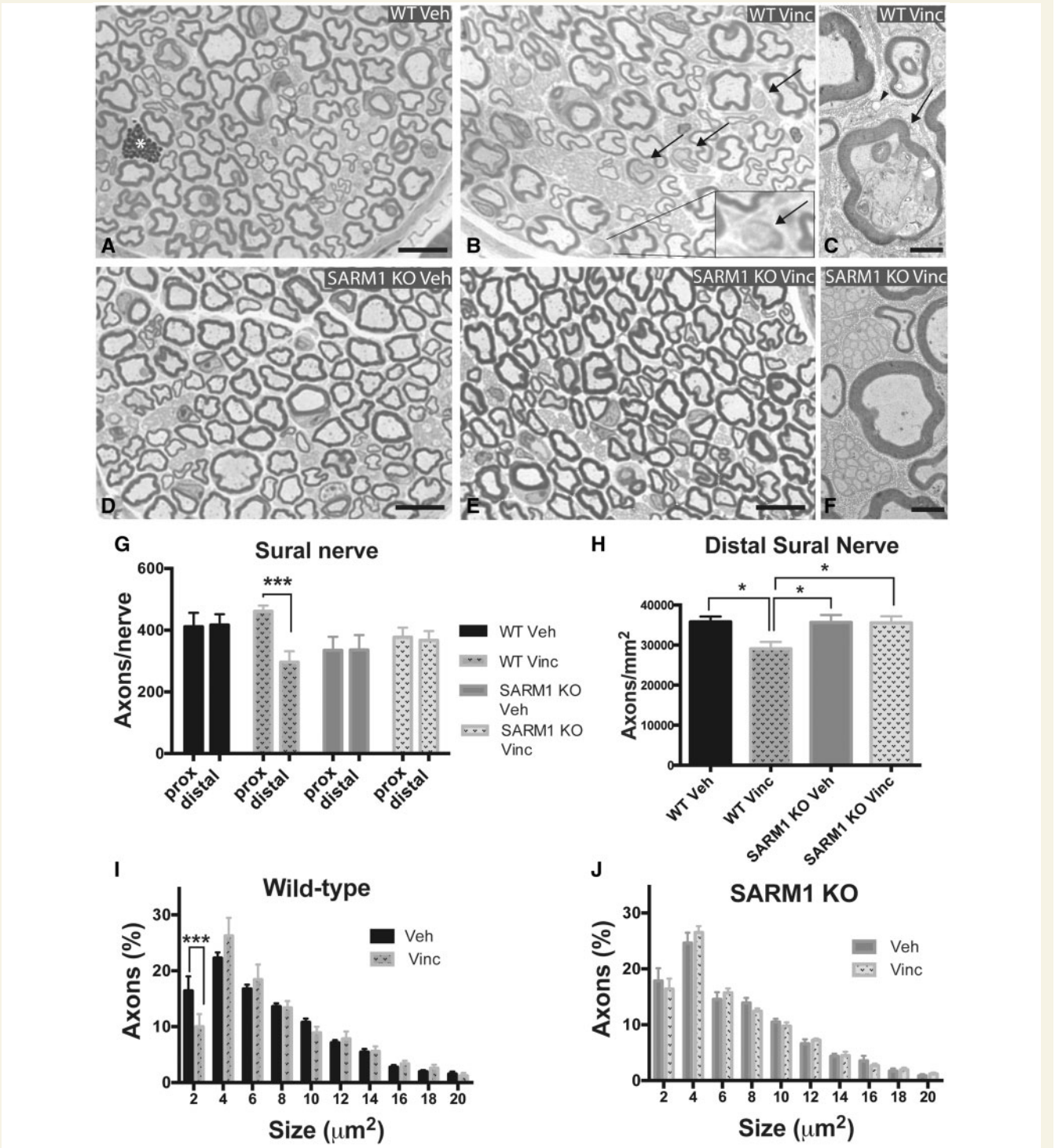

Figure 2 SARM1 knockout prevents degeneration of myelinated axons in the distal sural nerve in VIPN. (**A**, **B**, **D** and **E**) Photomicrographs of toluidine blue stained semithin cross sections of the distal sural nerve. There was no apparent difference in gross morphology between vehicle-treated wild-type (**A**) and SARM1 knockout (**D**) mice. In vincristine-treated wild-type mice, axons appear less densely packed (**B**). Some myelinated axons exhibit a homogenous pale or dark cytoplasm and disrupted myelin sheath (**B**, arrows, insert), likely representing degenerating axons. When axons with this morphology were evaluated at the electron microscopy level, they indeed show morphological signs of axonal degeneration (**C**, arrow). In contrast, distal sural nerves of vincristine-treated SARM1 knockout mice (**E**) look very similar to vehicle-treated sural nerves of SARM1 knockout mice. At the electron microscopy level, myelinated and unmyelinated axons of vincristine-treated SARM1 knockout mice appear morphologically intact (**F**). (**G**) When the same sural nerve is analysed at proximal and distal levels, there are significantly fewer axons distally in vincristine-treated wild-type mice, but not in vincristine-treated SARM1 knockout and vehicle-treated wild-type and SARM1 knockout mice [two-way repeated measures ANOVA, there was a significant main effect of genotype × proximal/distal localization $F(3,32) = 4.287$; $P = 0.0119$; Sidak's *post hoc* $^{***}P < 0.001$; $n = 7–12$ per group]. There was no difference in axon number of the

(continued)

Sensory symptoms of VIPN start in the fingertips and toes and often persist after discontinuation of vincristine (Boyette-Davis *et al.*, 2013). We therefore asked whether genetic deletion of SARM1 also protects from myelinated axon loss in the toes. To analyse these nerves, third toes were embedded and sectioned from the proximal end. Each toe typically contains three to five larger fascicles and a variable number of several small fascicles, some consisting of only 1–3 axons. We analysed axons in all fascicles that had a minimum fascicle size of 500 μm^2 (~20 axons). Vehicle-treated SARM1 knockout mice showed a trend toward fewer axons than wild-type mice, but this was not statistically significant (SARM1 knockout 48.5 ± 3, wild-type 53.9 ± 3; $P = 0.25$, unpaired t test, $n = 7$–11 per group). In vincristine-treated wild-type mice, we observed abundant axons with signs of axonal degeneration (Fig. 3B and E; $P < 0.0001$) and these mice had significantly fewer axons per fascicle than vehicle-treated wild-type mice [wild-type Veh 53.9 ± 3.1; wild-type Vinc 42.4 ± 3.22; one-way ANOVA (F3,37) = 3,402; $P = 0.028$; Tukey's multiple comparison test $P < 0.05$]. In contrast, axon numbers in vincristine-treated SARM1 knockout mice were not different from vehicle-treated SARM1 knockout mice (SARM1 knockout Veh 48.5 ± 3, SARM1 knockout Vinc 45.3 ± 1.6; not significant; $n = 7$–13 for all four groups) and mice did not exhibit many axons with signs of axonal degeneration (Fig. 3D and E). These results indicate that loss of SARM1 protects from vincristine-induced axonal degeneration in the toes.

VIPN in humans typically starts with sensory symptoms, but at higher dosages may also cause distal weakness (Bradley *et al.*, 1970; DeAngelis *et al.*, 1991; Haim *et al.*, 1994). We therefore analysed a motor nerve, i.e. the tibial nerve sectioned at the ankle. We found no differences in axon number in vehicle and vincristine-treated wild-type and SARM1 knockout mice (wild-type vehicle 1456 ± 15.5, wild-type vincristine 1397 ± 49.1, SARM1 knockout vehicle 1457 ± 11.2, SARM1 knockout vincristine 1451 ± 13; one-way ANOVA, not significant, $n = 9$–14 per group). Hence, our model does not induce a motor neuropathy. Taken together, these data demonstrate that we have established a distal, sensory predominant neuropathy with significant axon loss in the toe and distal sural nerve. In this model, loss of SARM1 blocks axonal degeneration.

Genetic deletion of SARM1 prevents the development of nerve conduction abnormalities following vincristine treatment

Many patients with VIPN show abnormalities on nerve conduction studies. To determine whether the axonal preservation seen in SARM1 knockout mice is associated with improved electrophysiological function, we performed nerve conduction studies of the tail. We analysed the CNAP amplitude and the conduction velocity, which reflect axon number and degree of myelination, respectively. Studies in patients treated with vincristine show an early decrease of sensory nerve action potentials, while the conduction velocity remains unchanged (Sandler *et al.*, 1969; Casey *et al.*, 1973; Guiheneuc *et al.*, 1980), consistent with an axonal neuropathy. Orthodromic stimulation of the tail nerves of isoflurane anaesthetized mice revealed a similar size, duration and morphology of the CNAP as well as conduction velocity in wild-type and SARM1 knockout mice at baseline (Fig. 4A and B). After vincristine treatment, there was a significant decrease in the CNAP amplitude in wild-type mice (Fig. 4A and C; $P < 0.01$). As in human studies, there was no decrease in conduction velocity (Fig. 4D). In SARM1 knockout mice, the morphology and size of the CNAP amplitude and the conduction velocity were not significantly different after vincristine treatment (Fig. 4A, C and D). Because the amplitude was slightly reduced following vincristine treatment there was no significant difference in amplitude between treated wild-type and SARM1 knockout mice. These findings support the contention that loss of SARM1 blocks the development of electrophysiological abnormalities caused by vincristine treatment, and are consistent with the anatomical data demonstrating preservation of axon number.

Genetic deletion of SARM1 blocks the development of hyperalgesia following vincristine treatment

In patients treated with vincristine, pain in the hands and feet may be an early sign of neuropathy. Subsequently, gait imbalance may develop and, typically at higher dosages, weakness in ankle dorsiflexion and wrist extension.

Figure 2 Continued

proximal sural nerve between vehicle and vincristine-treated wild-type and SARM1 knockout mice [one-way ANOVA, $F(3,32) = 2.736$, $P = 0.0597$]. (**H**) Vincristine treated wild-type mice have significantly decreased axon density in the distal sural nerve compared to vehicle-treated wild-type and SARM1 knockout mice as well as vincristine-treated SARM1 knockout mice [one-way ANOVA; $F(3,41) = 4.361$; $P = 0.0094$; Tukey's *post hoc* $^*P < 0.05$; $n = 9$–13 per group]. (**I** and **J**) Analysis of axon size of the distal sural nerve reveals a decrease in the proportion of small myelinated axons in vincristine-treated wild-type mice (**I**, multiple *t*-tests with Bonferroni correction; $^{***}P < 0.001$; $n = 9$–10), but not in vincristine-treated SARM1 knockout mice (**H**; multiple *t*-tests; $n = 8$–11). In **A**, the asterisk marks a granular cell; in **B** and **C**, arrows point to myelinated axons with signs of degeneration; in **C**, arrowhead points to a degenerating Remak bundle. **I** and **J** analysed to axon size of 38 μm, shown to size of 20 μm for clarity. Scale bar in **A**, **B**, **D**, and **E** = 10 μm; **C** and **F** = 2 μm. KO = knockout.

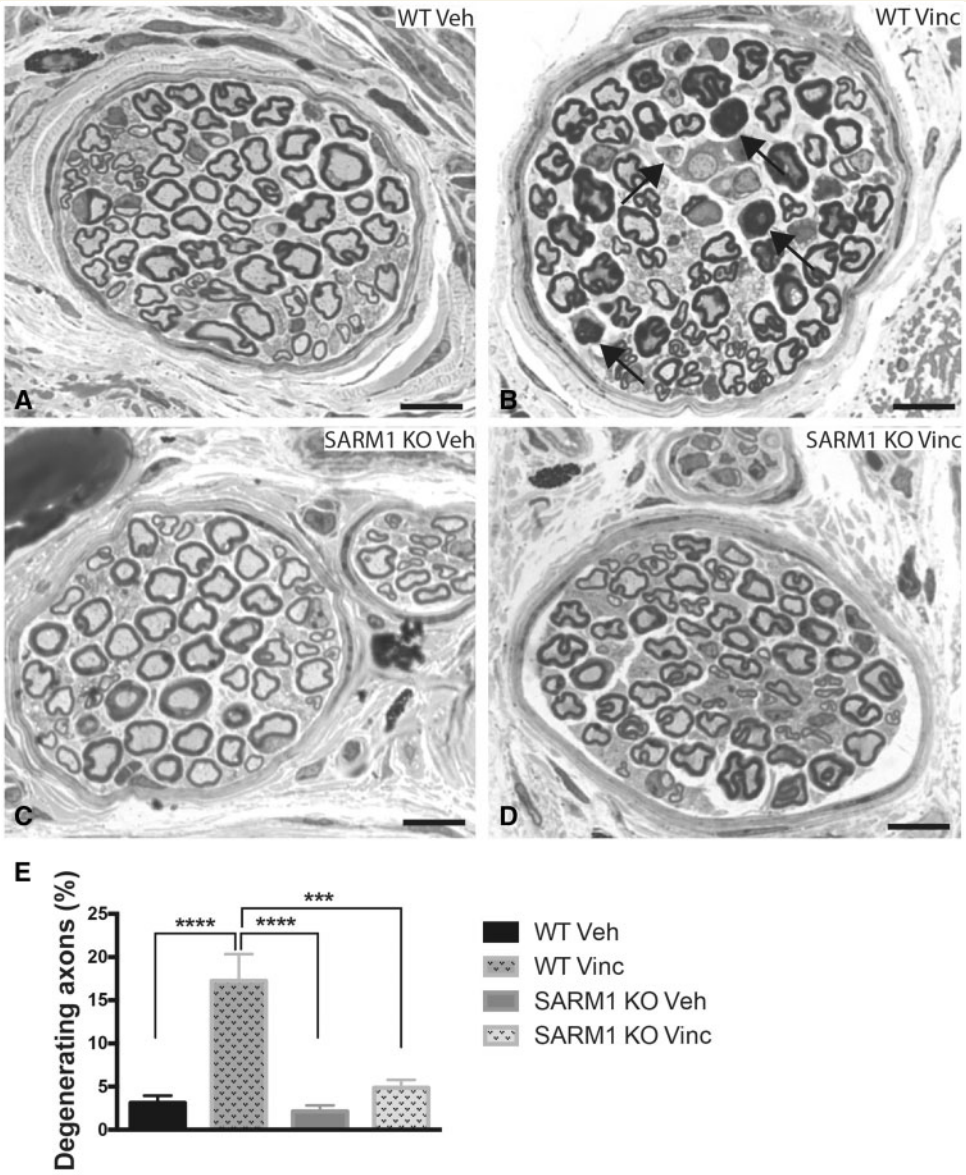

Figure 3 Genetic deletion of SARM1 blocks vincristine-induced axonal degeneration in nerve fascicles of the toe. (**A–D**) Photomicrographs of toluidine blue-stained semithin sections of nerve fascicles in the toe demonstrate morphological changes and axonal degeneration in vincristine-treated wild-type mice (**B**, arrows), whereas nerve fascicles of vincristine-treated SARM1 knockout (**D**) and vehicle-treated wild-type (**A**) and SARM1 knockout (**C**) appear morphologically similar. (**E**) There are significantly more axons with signs of degeneration in vincristine-treated wild-type mice when compared to vehicle-treated wild-type and SARM1 knockout as well as vincristine-treated SARM1 knockout mice [one-way ANOVA $F(3,40) = 13.34$; $P < 0.0001$; Tukey's multiple comparison test; ****$P < 0.0001$; ***$P < 0.001$, $n = 7$ for vehicle-treated wild-type and SARM1 knockout mice, $n = 13$ for vincristine-treated wild-type and SARM1 knockout mice]. For clarity in the figure, only significant results are indicated. Scale bar = 10 μm. KO = knockout.

Mouse models of vincristine-induced neuropathy are characterized by mechanical hyperalgesia (Authier *et al.*, 2003; Saika *et al.*, 2009; Boehmerle *et al.*, 2014; Shen *et al.*, 2015), sometimes heat hyperalgesia (Authier *et al.*, 2003; Kamei *et al.*, 2005) and rarely motor symptoms (Bruna *et al.*, 2011; Boehmerle *et al.*, 2014). We tested for the development of vincristine-induced changes in mechanical and heat sensitivity, gait imbalance (ataxia) and weakness by evaluating wild-type and SARM1 knockout mice before the first injection of vincristine and again 1 week after the last.

We evaluated vincristine-induced mechanical hyperalgesia in wild-type and SARM1 knockout mice using a graded series of von Frey filaments. At baseline there were no differences in the mechanical withdrawal thresholds between SARM1 knockout and wild-type mice (Fig. 5A). In line with previous studies (Authier *et al.*, 2003; Saika *et al.*, 2009; Boehmerle *et al.*, 2014), we observed a profoundly

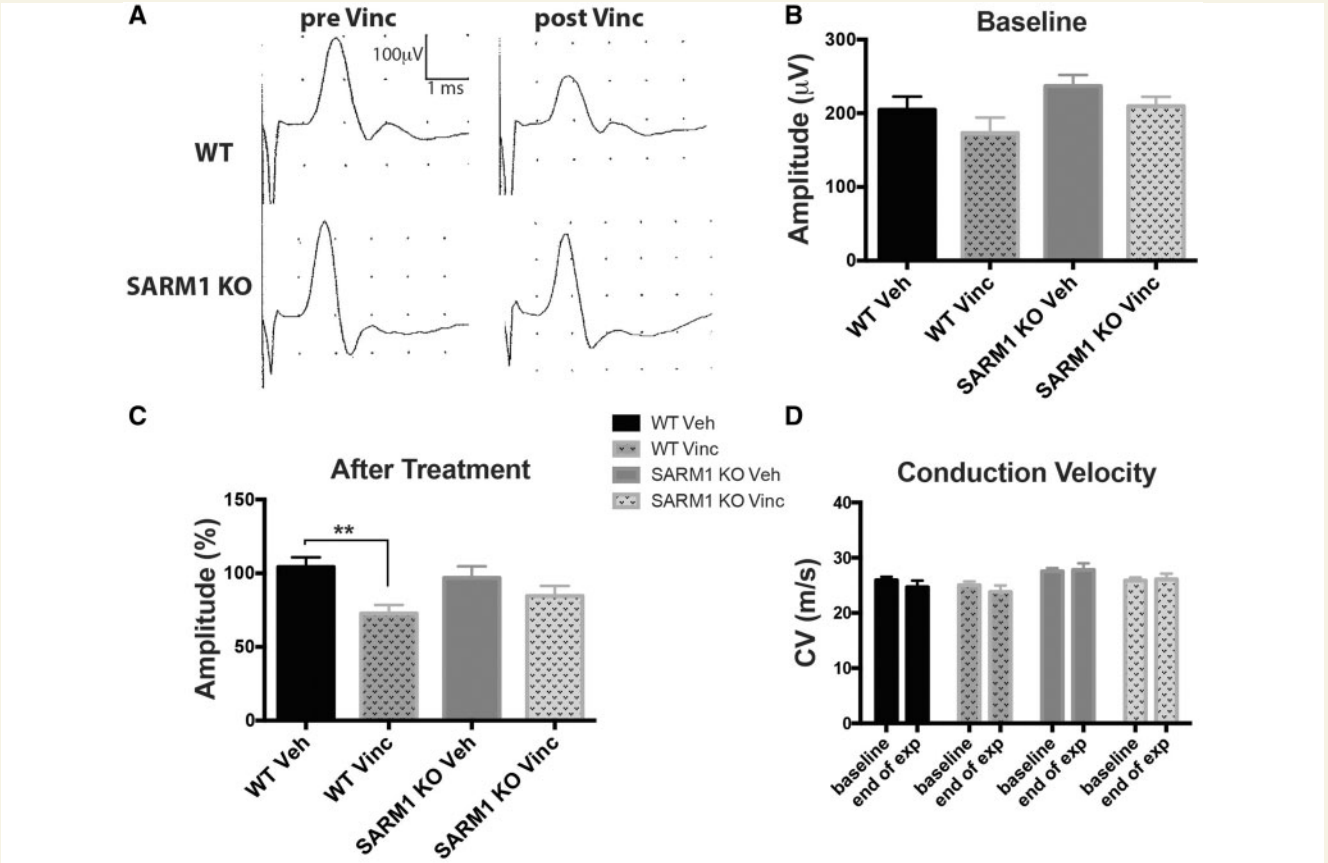

Figure 4 SARM1 knockout preserves the tail action potential amplitude following vincristine treatment. (**A**) Depicted are representative tracings from one wild-type and one SARM1 knockout mouse before and after vincristine. Note the decreased tail amplitude after vincristine treatment in wild-type, but not SARM1 knockout mice. (**B**) The tail amplitude is not statistically significantly different between groups at baseline [one-way ANOVA, $P = 0.1031$, $F(3,46) = 2.181$; $n = 10–15$ per group]. (**C**) After vincristine, wild-type mice show a decreased tail amplitude [one-way ANOVA, $P = 0.0091$ $F(3,46) = 4.325$, $^{**}P < 0.01$, Tukey's *post hoc*; $n = 10–15$ per group], whereas the tail amplitude of vincristine-treated SARM1 knockout mice is not significantly different. (**D**) There was no change in conduction velocity in any of the groups [two-way ANOVA, there was no significant main effect between groups $F(3,46) = 2.787$, $P = 0.0512$ and between pre and post vincristine treatment $F(1,46) = 0.9229$, $P = 0.3417$; $n = 10–15$ per group]. KO = knockout.

lowered withdrawal threshold after vincristine administration in wild-type mice (Fig. 5A; $P < 0.001$), indicating the development of vincristine-induced hyperalgesia. Remarkably, SARM1 knockout mice exhibited no significant change in the withdrawal threshold after vincristine when compared to baseline (Fig. 5A).

To evaluate for heat hyperalgesia, the temperature of an analgesia meter was increased at a constant rate from 31°C to 51°C and the temperature at which mice withdrew and licked their hind paws was recorded. Again, wild-type mice withdrew their paws at a slightly, but significantly, lower temperature after vincristine administration (Fig. 5B; $P < 0.01$) consistent with a hypersensitivity to heat. In contrast, the withdrawal threshold in vincristine-treated SARM1 knockout mice did not change when compared to baseline (Fig. 5B).

While in adult patients, changes in sensation occur early in the course of VIPN, at higher cumulative dosages gait imbalance and distal weakness may develop (Casey *et al.*, 1973; DeAngelis *et al.*, 1991). We assessed for ataxia by subjecting the mice to rotarod performance testing. To avoid the potential confound of differences in motor learning, we first established that mice would stay on the rotarod with slow constant speed for 2 min. We then evaluated the mice at constant and accelerating rotarod speeds before and after vincristine administration. There were no differences in any of the rotarod performances between wild-type or SARM1 knockout mice or between baseline and after vincristine treatment indicating that no group developed severe gait imbalance (Fig. 5C). Finally, we evaluated for development of weakness by measuring the time a mouse was able to hold on to a 180° inverted screen. There were no differences in the ability to hold on to the inverted screen before and after vincristine treatment in either wild-type or SARM1 knockout mice suggesting that no group developed appreciable weakness (Fig. 5D). These data also demonstrate that there was no impairment in motor performance, motivation, or overall decreased well-being that could account for the differences in mechanical and heat withdrawals between SARM1 knockout and wild-type mice.

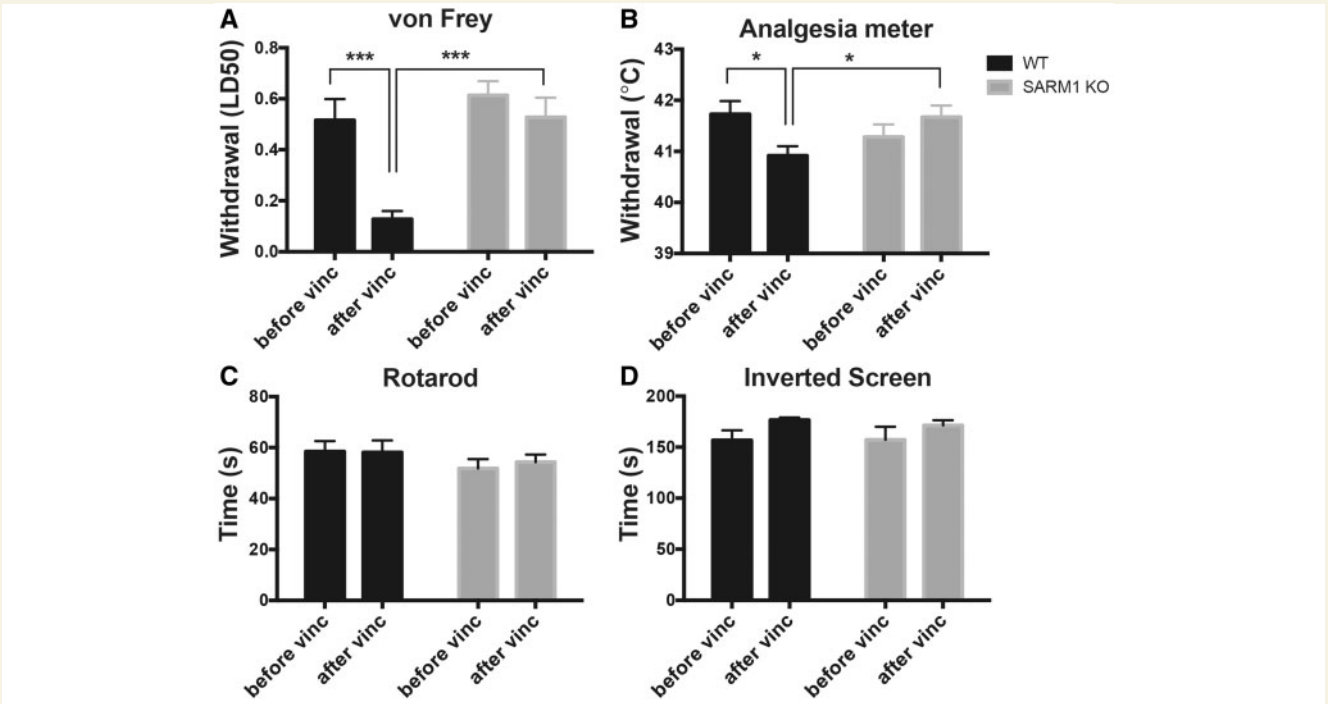

Figure 5 SARM1 knockout prevents the development of hyperalgesia in VIPN. (**A**) The mechanical withdrawal threshold is significantly reduced after vincristine in wild-type mice, but not in SARM1 knockout mice. There was a significant main effect between groups [two-way repeated measures ANOVA $F(1,15) = 9.718$; $P = 0.0071$), time $F(1,15) = 19.74$, $P < 0.0005$ and time × group interaction $F(1,15) = 8.035$, $P = 0.0126$; Sidak's multiple comparison test ***$P < 0.001$ $n = 7$–10 per group]. (**B**) After vincristine treatment, the heat withdrawal threshold decreases significantly in wild-type mice, but not SARM1 knockout mice [two-way repeated measures ANOVA, significant main effect on time × genotype interaction $F(1,15) = 10.69$; $P = 0.0052$; Sidak's *post hoc* *$P < 0.05$; $n = 7$–10 per group]. (**C**) There was no difference in rotarod performance in any of the groups (two-way repeated measures ANOVA, there was no main effect between groups, time and group × time interaction). (**D**) There was no difference in the time mice are able to hang on to an inverted screen between wild-type and SARM1 knockout mice (two-way repeated measures ANOVA, $n = 7$–10 per group). KO = knockout.

Taken together, our VIPN model mirrors moderately severe vincristine-induced neuropathy, as shown by hyperalgesia, abnormalities in nerve conduction studies, and degeneration of intraepidermal nerve fibres and distal myelinated axons. Genetic deletion of SARM1 blocks all of these sequelae of vincristine treatment. Hence, SARM1 is necessary for the development of VIPN in mice. Moreover, these findings show that SARM1 promotes axon loss in a chronic, subacute degeneration model, suggesting that inhibition of SARM1 or its downstream effectors may be useful therapeutically in chemotherapy-induced peripheral neuropathies such as VIPN and potentially more broadly in degenerative diseases characterized by axon loss.

Discussion

Establishment of a vincristine-induced peripheral neuropathy model in mice

Vincristine is one of the most widely used and effective anticancer agents for treating leukaemias, lymphomas, brain tumours and solid tumours in adults and children. Vincristine acts by inhibiting microtubule polymerization thereby preventing mitotic spindle formation, but also affects axonal microtubules and so impairs anterograde and retrograde axonal transport (LaPointe *et al.*, 2013). This defect in axonal transport is a likely trigger for peripheral neuropathy, which is a common and often dose-limiting side effect of vincristine. Most patients treated with vincristine develop a dose-dependent peripheral polyneuropathy with sensory symptoms beginning at a cumulative dose of 5 mg and motor symptoms developing at higher doses around 30–50 mg (Casey *et al.*, 1973).

Electrodiagnostic and histomorphological evaluations demonstrate that VIPN is a distal axonopathy, characterized by loss of distal myelinated axons (Moress *et al.*, 1967; Gottschalk *et al.*, 1968; Bradley *et al.*, 1970; Casey *et al.*, 1973; Guiheneuc *et al.*, 1980). Here, we have developed a mouse model of VIPN that mimics features of the human disease. Upon vincristine treatment of wild-type mice, nerve conduction studies reveal an axonal neuropathy, with a decrease in action potential amplitude without a change in conduction velocity. This finding is confirmed in our histological analysis demonstrating a loss of myelinated axons in nerves innervating the toe as well as in the

distal sural nerve. We directly demonstrate that this is a distal predominant axon loss—there is preferential loss of axons in the distal sural compared to proximal sural nerve from the same treated animals. A similar observation has been made from human autopsy material in which primary axonal degeneration was found in the sural nerve, but not in the proximal sciatic nerves, nerve roots, dorsal root ganglion neurons or spinal cord (Moress *et al.*, 1967; Bradley *et al.*, 1970). We did not detect axonal degeneration in the distal tibial nerve, which is a motor nerve, and consistent with this found no motor abnormalities in these mice.

Pain can be an early and especially disabling symptom of VIPN. In a study of 128 children who were treated with vincristine for leukaemia, 44% of patients reported VIPN-associated pain (Lavoie Smith *et al.*, 2015). In rodent models of VIPN, pain and hyperalgesia are commonly demonstrated (Authier *et al.*, 2003; Saika *et al.*, 2009; Boehmerle *et al.*, 2014; Shen *et al.*, 2015) and are associated with decreased intraepidermal nerve fibre density (Siau *et al.*, 2006). Consistent with these findings, our wild-type mice developed pronounced mechanical hyperalgesia and allodynia and mild, but significant, heat hyperalgesia. The intraepidermal nerve fibre density was significantly reduced and remaining fibres in the epidermis were shorter, indicating prominent involvement of small nerve fibres in our VIPN model.

Although pain and allodynia are frequently associated with loss of intraepidermal nerve density, as we also observed in our study, mechanisms underlying this apparent paradox are not fully understood, but likely include changes in both peripheral and central nervous systems. In rodent models of VIPN, C-fibres become hyper-responsive to innocuous mechanical and heat stimulation (Tanner *et al.*, 1998*b*, 2003) and wide dynamic range neurons in the spinal cord exhibit increased spontaneous activity (Weng *et al.*, 2003). These changes are accompanied by structural and molecular alterations in neurons and primary afferent fibres in the spinal dorsal horn (Thibault *et al.*, 2013). Although to the best of our knowledge it has not been demonstrated directly which C-fibres become hyper-responsive after vincristine, in other nerve injury models hyper-responsiveness was found in both damaged C-fibres and undamaged axons (Wu *et al.*, 2001, 2002). It is hypothesized that Schwann cells of Remak bundles may respond to denervation by release of glial cell derived factors that change the spontaneous activity and responsiveness of neighbouring intact C-fibres (Wu *et al.*, 2001). While mice did develop increased pain sensitivity in our VIPN model, we did not observe a numbness phenotype in our mice, which is in line with other mouse and rat studies of VIPN (Saika *et al.*, 2009; Boehmerle *et al.*, 2014). We hypothesize that the prominent allodynia observed in our and other studies masks evaluation of subtle numbness.

In all of our studies, experimental groups were heterogeneous, consisting of males and females between 12 and 31 weeks old at the beginning of the experiment (mean 20 ± 0.4 weeks). Although this range was necessitated by the inherent challenges of working with genetic models, it shows that our results are robust and are not restricted to a specific gender or age. Thus, we have generated a clinically relevant model of VIPN in mice that mimics the behavioural, electrophysiological, and anatomical defects observed in mild to moderate, sensory predominant VIPN in humans.

SARM1 is required for the development of VIPN

Remarkably, genetic deletion of SARM1 prevents the development of all of the hallmarks of neuropathy in vincristine-treated mice. On treatment, the SARM1 knockout mice do not have a decrease in nerve action potential amplitude, do not lose myelinated axons or intraepidermal nerve fibres, and do not develop hyperalgesia. Thus, we conclude that SARM1 is necessary for the development of VIPN. We demonstrate for the first time that axon loss can be blocked in an *in vivo* model of VIPN and that this is associated with improved functional outcome. This indicates that neuroprotective strategies may be useful to prevent the development of chemotherapy-induced peripheral neuropathies.

Although we used a whole body SARM1 knockout mouse, the observed axonal protection in SARM1 knockout mice is most likely due to SARM1's action in nerves. SARM1 is almost exclusively expressed in the nervous system. In three previous studies SARM1 was detected at high levels in the brain and at low levels in lymph nodes and spleen. SARM1 was not detectable in kidney, liver, lung, heart, skeletal muscle, testis, thymus, monocytes, polymorphonuclear leucocytes and bone marrow derived macrophages of normal human and mouse tissues (Kim *et al.*, 2007; Szretter *et al.*, 2009; Chen *et al.*, 2011). Because *in vitro* experiments on dorsal root ganglion neurons show that SARM1 acts neuron- and axon-autonomously and lymphocytes have not been shown to play a prominent role in inducing axon loss in vincristine-induced neuropathy, it is likely that most if not all of the axo-protective effect of our SARM1 knockout is due to its action in axons. This notion is also supported by similarities in responses between SARM1 knockout and wild-type mice to other effects of vincristine treatment, such as weight loss, hair loss and mortality.

Mortality in rodent models of VIPN is not uncommon and the mortality in our mice is similar to or less than in that reported in previously published rodent models of VIPN (Bruna *et al.*, 2011). As a microtubule inhibitor, vincristine affects many systems in the body. In addition to neuropathy, vincristine may cause, among others, alopecia, myelosuppression, nephropathy, bronchospasm and myocardial infarction. The cause of mortality in mice is not known, but may be multifactorial. Intravenous infusions of vincristine in human patients are typically relatively

well tolerated and are not associated with increased mortality. The fact that SARM1 knockout prevented neuropathy, but had no effect on mortality, weight loss and alopecia, supports the hypothesis that SARM1 only mediates the neuropathic side effects of vincristine treatment.

How might SARM1 be activated in distal axonopathies such as VIPN and why does only the most distal part of the axon degenerate? Clues come from Wallerian degeneration. In Wallerian degeneration, the SARM1 pathway is likely activated by the consequences of the loss of the axonal survival factor NMNAT2. NMNAT2 is essential for axon survival, as the loss of NMNAT2 is sufficient to induce SARM1-dependent axonal degeneration in the absence of axonal injury (Gilley and Coleman, 2010; Gilley *et al.*, 2015). NMNAT2 is a labile protein with a short half-life that must constantly be delivered to the axon via anterograde transport from the cell body (Milde *et al.*, 2013). After axotomy, axonal transport is blocked and NMNAT2 is rapidly depleted, which likely activates the SARM1 pathway and triggers the axonal degeneration pathway (reviewed in Gerdts *et al.*, 2016). In VIPN, axonal transport is also impaired, but not blocked (LaPointe *et al.*, 2013). This likely leads to a more profound loss of NMNAT2 distally, activating the SARM1 pathway locally. In this model, residual axonal transport is sufficient to maintain NMNAT2 in proximal axons at levels that block SARM1 pathway activation, thereby restricting degeneration to the distal axon.

SARM1 as a therapeutic target for preventing axonal neuropathies such as VIPN

Although most patients report some improvement in symptoms after discontinuation of vincristine, VIPN related peripheral neuropathy persists in many patients for years after completing their chemotherapy and can persist for decades (Boyette-Davis *et al.*, 2013; Liew *et al.*, 2013; Ness *et al.*, 2013). With longer disease-free intervals, quality of life concerns become increasingly important in the evaluation of potential chemotherapeutic regimens. There are no specific treatments to prevent VIPN or any chemotherapy-induced peripheral neuropathy. For vincristine, neurotoxic effects are minimized by setting an arbitrary upper limit (e.g. 2 mg) on single vincristine doses and by modifying or delaying additional doses during the course of treatment. VIPN is especially severe if patients have a pre-existing neuropathy (Chaudhry *et al.*, 2003) or a condition that predisposes them to develop neuropathy (e.g. diabetes mellitus). Given the effectiveness of vincristine to treat cancers and because dose intensity of vincristine positively correlates with complete response and survival (DeAngelis *et al.*, 1991), prevention or amelioration of neurotoxic complications would be preferable to dose reduction. Several attempts to limit vinca alkaloid neuropathy have been made, including liposomal encapsulation, administration of continuous infusion rather than bolus injection, development of non-neurotoxic analogues and treatment with neuroprotective drugs. However, success has been limited and dose limits and reductions remain the mainstay to decrease neurotoxic effects. Notably, none of these measures target the underlying mechanism of axonal degeneration.

Here we show that axonal degeneration in VIPN is mediated by SARM1. Hence SARM1 not only mediates axon destruction in response to acute injuries such as axotomy and traumatic brain injury, but also in the setting of chronic axon loss in a neuropathy. While we have modelled vincristine-induced peripheral neuropathy, our findings are consistent with the view that the SARM1 axon destruction pathway mediates axon loss in other neuropathies and potentially in other neurodegenerative diseases in which axon loss is an early and important event. Development of therapeutics targeting the SARM1 pathway may provide new treatment options for these devastating disorders.

Recent advances in our understanding of the SARM1 mechanism of action raise hopes that such therapeutics can be developed. Activation of the SARM1 pathway rapidly depletes NAD^+, which is quickly followed by loss of ATP, and subsequently by morphological degeneration of the axon (Gerdts *et al.*, 2015). Maintaining NAD^+ is sufficient to block SARM1-induced axonal degeneration *in vitro* (Gerdts *et al.*, 2015). Conversely, pharmacologically depleting NAD^+ by other means can bypass the requirement for SARM1 in axon destruction. Thus, maintaining NAD^+ by boosting NAD^+ synthesis or blocking NAD^+ destruction may be valuable therapeutic strategies. Indeed, axon destruction induced by a constitutively active form of SARM1 is blocked *in vitro* by expression of the NAD^+ synthesizing enzymes NMNAT1 and NAMPT or by supplementation with the NAD^+ precursor nicotinamide riboside (Gerdts *et al.*, 2015), which is a form of vitamin B3 that readily enters the cell and has no known adverse effects. Therefore, nicotinamide riboside may be a promising therapeutic option to decrease axonal degeneration in VIPN and other chemotherapy-induced peripheral neuropathies. Furthermore, P7C3, which may increase NAD^+ by activating NAMPT (Wang *et al.*, 2014), decreases axonal degeneration in rodent models of amyotrophic lateral sclerosis, Parkinson's disease and traumatic brain injury (De Jesus-Cortes *et al.*, 2012; Tesla *et al.*, 2012; Yin *et al.*, 2014). While these are exciting possibilities, boosting NAD^+ synthesis would still compete with SARM1 pathway activation and ongoing NAD^+ destruction. It is currently not known how SARM1 is activated and whether SARM1 possesses NADase activity or activates an NAD^+ consuming enzyme. Defining the mechanism of SARM1 activation and NAD^+ destruction may identify novel therapeutic targets to block axonal degeneration and treat neuropathies and other diseases of axon loss.

Acknowledgements

We thank Judy Golden for training and advice regarding the von Frey experiments, Elizabeth Streif and Glenn Lopate for staining protocol and advice regarding PGP9.5 staining, and Susan Mackinnon and Daniel Hunter for use of the Leica UC6 ultramicrotome. Electron microscopy was performed through the use of Washington University Center for Cellular Imaging (WUCCI).

Funding

This study was funded by a Clinical Research Training Fellowship from the American Brain Foundation and K08NS091448 to S.G., a Foundation for Barnes Jewish Hospital Cancer Frontier Fund and Siteman Cancer Center grant to A.D. and J.M., the NIH NS087632 to J.M. and A.D and a microgrant from the Children's Discovery Institute to A.D.

Supplementary material

Supplementary material is available at *Brain* online.

References

Araki T, Sasaki Y, Milbrandt J. Increased nuclear NAD biosynthesis and SIRT1 activation prevent axonal degeneration. Science 2004; 305: 1010–3.

Argyriou AA, Kyritsis AP, Makatsoris T, Kalofonos HP. Chemotherapy-induced peripheral neuropathy in adults: a comprehensive update of the literature. Cancer Manag Res 2014; 6: 135–47.

Authier N, Gillet J-P, Fialip J, Eschalier A, Coudore F. A new animal model of vincristine-induced nociceptive peripheral neuropathy. Neurotoxicology 2003; 24: 797–805.

Beirowski B, Adalbert R, Wagner D, Grumme DS, Addicks K, Ribchester RR, et al. The progressive nature of Wallerian degeneration in wild-type and slow Wallerian degeneration (WldS) nerves. BMC Neurosci 2005; 6: 1–27.

Boehmerle W, Huehnchen P, Peruzzaro S, Balkaya M, Endres M. Electrophysiological, behavioral and histological characterization of paclitaxel, cisplatin, vincristine and bortezomib-induced neuropathy in C57Bl/6 mice. Sci Rep 2014; 4: 6370.

Boyette-Davis JA, Cata JP, Driver LC, Novy DM, Bruel BM, Mooring DL, et al. Persistent chemoneuropathy in patients receiving the plant alkaloids paclitaxel and vincristine. Cancer Chemother Pharmacol 2013; 71: 619–26.

Bradley WG, Lassman LP, Pearce GW, Walton JN. The neuromyopathy of vincristine in man. Clinical, electrophysiological and pathological studies. J Neurol Sci 1970; 10: 107–31.

Bruna J, Alé A, Velasco R, Jaramillo J, Navarro X, Udina E. Evaluation of pre-existing neuropathy and bortezomib retreatment as risk factors to develop severe neuropathy in a mouse model. J Peripher Nerv Syst 2011; 16: 199–212.

Carozzi VA, Canta A, Chiorazzi A. Chemotherapy-induced peripheral neuropathy: What do we know about mechanisms? Neurosci Lett 2015; 596: 90–107.

Casey EB, Jellife AM, Le Quesne PM, Millett YL. Vincristine neuropathy. Clinical and electrophysiological observations. Brain 1973; 96: 69–86.

Chaplan SR, Bach FW, Pogrel JW, Chung JM, Yaksh TL. Quantitative assessment of tactile allodynia in the rat paw. J Neurosci Methods 1994; 53: 55–63.

Chaudhry V, Chaudhry M, Crawford TO, Simmons-O'Brien E, Griffin JW. Toxic neuropathy in patients with pre-existing neuropathy. Neurology 2003; 60: 337–40.

Chen CY, Lin CW, Chang CY, Jiang ST, Hsueh YP. Sarm1, a negative regulator of innate immunity, interacts with syndecan-2 and regulates neuronal morphology. J Cell Biol 2011; 193: 769–84.

Coleman MP, Conforti L, Buckmaster EA, Tarlton A, Ewing RM, Brown MC, et al. An 85-kb tandem triplication in the slow Wallerian degeneration (Wld(s)) mouse. Proc Natl Acad Sci USA 1998; 95: 9985–90.

Costa TC, Lopes M, Anjos AC, Zago MM. Chemotherapy-induced peripheral neuropathies: an integrative review of the literature. Rev Esc Enferm USP 2015; 49: 335–45.

De Jesus-Cortes H, Xu P, Drawbridge J, Estill SJ, Huntington P, Tran S, et al. Neuroprotective efficacy of aminopropyl carbazoles in a mouse model of Parkinson disease. Proc Natl Acad Sci USA 2012; 109: 17010–5.

DeAngelis LM, Gnecco C, Taylor L, Warrell RP Jr. Evolution of neuropathy and myopathy during intensive vincristine/corticosteroid chemotherapy for non-Hodgkin's lymphoma. Cancer 1991; 67: 2241–6.

Diouf B, Crews KR, Lew G, Pei D, Cheng C, Bao J, et al. Association of an inherited genetic variant with vincristine-related peripheral neuropathy in children with acute lymphoblastic leukemia. JAMA 2015; 313: 815–23.

Dixon WJ. Efficient analysis of experimental observations. Annu Rev Pharmacol Toxicol 1980; 20: 441–62.

Ebenezer GJ, McArthur JC, Thomas D, Murinson B, Hauer P, Polydefkis M, et al. Denervation of skin in neuropathies: the sequence of axonal and Schwann cell changes in skin biopsies. Brain 2007; 130(Pt 10): 2703–14.

Ezendam NP, Pijlman B, Bhugwandass C, Pruijt JF, Mols F, Vos MC, et al. Chemotherapy-induced peripheral neuropathy and its impact on health-related quality of life among ovarian cancer survivors: results from the population-based PROFILES registry. Gynecol Oncol 2014; 135: 510–7.

Gerdts J, Brace EJ, Sasaki Y, DiAntonio A, Milbrandt J. SARM1 activation triggers axon degeneration locally via NAD(+) destruction. Science 2015; 348: 453–7.

Gerdts J, Summers DW, Milbrandt J, DiAntonio A. Axon self-destruction: new links among SARM1, MAPKs, and NAD+ metabolism. Neuron 2016; 89: 449–60.

Gerdts J, Summers DW, Sasaki Y, DiAntonio A, Milbrandt J. Sarm1-mediated axon degeneration requires both SAM and TIR interactions. J Neurosci 2013; 33: 13569–80.

Gilley J, Coleman MP. Endogenous Nmnat2 is an essential survival factor for maintenance of healthy axons. PLoS Biol 2010; 8: e1000300.

Gilley J, Orsomando G, Nascimento-Ferreira I, Coleman MP. Absence of SARM1 rescues development and survival of NMNAT2-deficient axons. Cell Rep 2015; 10: 1974–81.

Gottschalk PG, Dyck PJ, Kiely JM. Vinca alkaloid neuropathy: nerve biopsy studies in rats and in man. Neurology 1968; 18: 875–82.

Guiheneuc P, Ginet J, Groleau JY, Rojouan J. Early phase of vincristine neuropathy in man. Electrophysiological evidence for a dying-back phenomenon, with transitory enhancement of spinal transmission of the monosynaptic reflex. J Neurol Sci 1980; 45: 355–66.

Haim N, Epelbaum R, Ben-Shahar M, Yarnitsky D, Simri W, Robinson E. Full dose vincristine (without 2-mg dose limit) in the treatment of lymphomas. Cancer 1994; 73: 2515–9.

Henninger N, Bouley J, Sikoglu EM, An J, Moore CM, King JA, et al. Attenuated traumatic axonal injury and improved functional

outcome after traumatic brain injury in mice lacking Sarm1. Brain 2016; 139(Pt 4): 1094–105.

Himes RH, Kersey RN, Heller-Bettinger I, Samson FE. Action of the vinca alkaloids vincristine, vinblastine, and desacetyl vinblastine amide on microtubules *in vitro*. Cancer Res 1976; 36: 3798–802.

Jongen JL, Broijl A, Sonneveld P. Chemotherapy-induced peripheral neuropathies in hematological malignancies. J Neurooncol 2015; 121: 229–37.

Kamei J, Tamura N, Saitoh A. Possible involvement of the spinal nitric oxide/cGMP pathway in vincristine-induced painful neuropathy in mice. Pain 2005; 117: 112–20.

Kim Y, Zhou P, Qian L, Chuang JZ, Lee J, Li C, et al. MyD88-5 links mitochondria, microtubules, and JNK3 in neurons and regulates neuronal survival. J Exp Med 2007; 204: 2063–74.

LaPointe NE, Morfini G, Brady ST, Feinstein SC, Wilson L, Jordan MA. Effects of eribulin, vincristine, paclitaxel and ixabepilone on fast axonal transport and kinesin-1 driven microtubule gliding: implications for chemotherapy-induced peripheral neuropathy. Neurotoxicology 2013; 37: 231–9.

Lavoie Smith EM, Li L, Chiang C, Thomas K, Hutchinson RJ, Wells EM, et al. Patterns and severity of vincristine-induced peripheral neuropathy in children with acute lymphoblastic leukemia. J Peripher Nerv Syst 2015; 20: 37–46.

Liew E, Thyagu S, Atenafu EG, Alibhai SM, Brandwein JM. Quality of life following completion of treatment for adult acute lymphoblastic leukemia with a pediatric-based protocol. Leuk Res 2013; 37: 1632–5.

Lin CW, Hsueh YP. Sarm1, a neuronal inflammatory regulator, controls social interaction, associative memory and cognitive flexibility in mice. Brain Behav Immun 2014; 37: 142–51.

Lunn ER, Perry VH, Brown MC, Rosen H, Gordon S. Absence of Wallerian degeneration does not hinder regeneration in peripheral nerve. Eur J Neurosci 1989; 1: 27–33.

Mack TG, Reiner M, Beirowski B, Mi W, Emanuelli M, Wagner D, et al. Wallerian degeneration of injured axons and synapses is delayed by a Ube4b/Nmnat chimeric gene. Nat Neurosci 2001; 4: 1199–206.

Massoll C, Mando W, Chintala SK. Excitotoxicity upregulates SARM1 protein expression and promotes Wallerian-like degeneration of retinal ganglion cells and their axons. Invest Ophthalmol Vis Sci 2013; 54: 2771–80.

Milde S, Gilley J, Coleman MP. Subcellular localization determines the stability and axon protective capacity of axon survival factor Nmnat2. PLoS Biol 2013; 11: e1001539.

Moress GR, D'Agostino AN, Jarcho LW. Neuropathy in lymphoblastic leukemia treated with vincristine. Arch Neurol 1967; 16: 377–84.

Ness KK, Jones KE, Smith WA, Spunt SL, Wilson CL, Armstrong GT, et al. Chemotherapy-related neuropathic symptoms and functional impairment in adult survivors of extracranial solid tumors of childhood: results from the St. Jude Lifetime Cohort Study. Arch Phys Med Rehabil 2013; 94: 1451–7.

Osterloh JM, Yang J, Rooney TM, Fox AN, Adalbert R, Powell EH, et al. dSarm/Sarm1 is required for activation of an injury-induced axon death pathway. Science 2012; 337: 481–4.

Owellen RJ, Hartke CA, Dickerson RM, Hains FO. Inhibition of tubulin-microtubule polymerization by drugs of the Vinca alkaloid class. Cancer Res 1976; 36: 1499–502.

Reinders-Messelink HA, Van Weerden TW, Fock JM, Gidding CE, Vingerhoets HM, Schoemaker MM, et al. Mild axonal neuropathy of children during treatment for acute lymphoblastic leukaemia. Eur J Paediatr Neurol 2000; 4: 225–33.

Saika F, Kiguchi N, Kobayashi Y, Fukazawa Y, Maeda T, Ozaki M, et al. Suppressive effect of imipramine on vincristine-induced mechanical allodynia in mice. Biol Pharm Bull 2009; 32: 1231–4.

Sandler SG, Tobin W, Henderson ES. Vincristine-induced neuropathy. A clinical study of fifty leukemic patients. Neurology 1969; 19: 367–74.

Shen Y, Zhang ZJ, Zhu MD, Jiang BC, Yang T, Gao YJ. Exogenous induction of HO-1 alleviates vincristine-induced neuropathic pain by reducing spinal glial activation in mice. Neurobiol Dis 2015; 79: 100–10.

Siau C, Xiao W, Bennett GJ. Paclitaxel- and vincristine-evoked painful peripheral neuropathies: loss of epidermal innervation and activation of Langerhans cells. Exp Neurol 2006; 201: 507–14.

Szretter KJ, Samuel MA, Gilfillan S, Fuchs A, Colonna M, Diamond MS. The immune adaptor molecule SARM modulates tumor necrosis factor alpha production and microglia activation in the brainstem and restricts West Nile Virus pathogenesis. J Virol 2009; 83: 9329–38.

Tanner KD, Levine JD, Topp KS. Microtubule disorientation and axonal swelling in unmyelinated sensory axons during vincristine-induced painful neuropathy in rat. J Comp Neurol 1998a; 424: 563–76.

Tanner KD, Reichling DB, Gear RW, Paul SM, Levine JD. Altered temporal pattern of evoked afferent activity in a rat model of vincristine-induced painful peripheral neuropathy. Neuroscience 2003; 118: 809–17.

Tanner KD, Reichling DB, Levine JD. Nociceptor hyper-responsiveness during vincristine-induced painful peripheral neuropathy in the rat. J Neurosci 1998b; 18: 6480–91.

Tesla R, Wolf HP, Xu P, Drawbridge J, Estill SJ, Huntington P, et al. Neuroprotective efficacy of aminopropyl carbazoles in a mouse model of amyotrophic lateral sclerosis. Proc Natl Acad Sci USA 2012; 109: 17016–21.

Thibault K, Rivals I, M'Dahoma S, Dubacq S, Pezet S, Calvino B. Structural and molecular alterations of primary afferent fibres in the spinal dorsal horn in vincristine-induced neuropathy in rat. J Mol Neurosci 2013; 51: 880–92.

Topp KS, Tanner KD, Levine JD. Damage to the cytoskeleton of large diameter sensory neurons and myelinated axons in vincristine-induced painful peripheral neuropathy in the rat. J Comp Neurol 2000; 424: 563–76.

Uceyler N, Braunsdorf S, Kunze E, Riediger N, Scheytt S, Divisova S, et al. Cellular infiltrates in skin and sural nerve of patients with polyneuropathies. Muscle Nerve 2016, Jul 7 Epub ahead of print.

Verstappen CC, Koeppen S, Heimans JJ, Huijgens PC, Scheulen ME, Strumberg D, et al. Dose- related vincristine-induced peripheral neuropathy with unexpected off-therapy worsening. Neurology 2005; 64: 1076–7.

Wang G, Han T, Nijhawan D, Theodoropoulos P, Naidoo J, Yadavalli S, et al. P7C3 neuroprotective chemicals function by activating the rate-limiting enzyme in NAD salvage. Cell 2014; 158: 1324–34.

Wang JT, Medress ZA, Barres BA. Axon degeneration: molecular mechanisms of a self-destruction pathway. J Cell Biol 2012; 196: 7–18.

Wang MS, Davis AA, Culver DG, Glass JD. WldS mice are resistant to paclitaxel (taxol) neuropathy. Ann Neurol 2002; 52: 442–7.

Wang MS, Fang G, Culver DG, Davis AA, Rich MM, Glass JD. The WldS protein protects against axonal degeneration: A model of gene therapy for peripheral neuropathy. Ann Neurol 2001; 50: 773–9.

Weng HR, Cordella JV, Dougherty PM. Changes in sensory processing in the spinal dorsal horn accompany vincristine-induced hyperalgesia and allodynia. Pain 2003; 103: 131–8.

Wu G, Ringkamp M, Hartke TV, Murinson BB, Campbell JN, Griffin JW, et al. Early onset of spontaneous activity in uninjured C-fiber nociceptors after injury to neighboring nerve fibers. J Neurosci 2001; 21: RC140.

Wu G, Ringkamp M, Murinson BB, Pogatzki EM, Hartke TV, Weerahandi HM, et al. Degeneration of myelinated efferent fibers induces spontaneous activity in uninjured C-fiber afferents. J Neurosci 2002; 22: 7746–53.

Yang J, Wu Z, Renier N, Simon DJ, Uryu K, Park DS, et al. Pathological axonal death through a MAPK cascade that triggers a local energy deficit. Cell 2015; 160: 161–76.

Yin TC, Britt JK, De Jesus-Cortes H, Lu Y, Genova RM, Khan MZ, et al. P7C3 neuroprotective chemicals block axonal degeneration and preserve function after traumatic brain injury. Cell Rep 2014; 8:1731–40.